HYDROLOGICAL PROCESSES
Hydrol. Process. **14**, 2711–2730 (2000)

Runoff generation in a hypermaritime bog–forest upland

J. J. Gibson,[1]* J. S. Price,[1] R. Aravena,[2] D. F. Fitzgerald[1] and D. Maloney[3]
[1]*Department of Geography and Wetlands Research Centre, University of Waterloo, Waterloo, ON, N2L 3G1, Canada*
[2]*Department of Earth Sciences, University of Waterloo, Waterloo, ON, N2L 3G1, Canada*
[3]*British Columbia Ministry of Forests, Smithers, BC, Canada*

Abstract:

Shallow hillslope groundwater is shown to be a dominant source of streamflow in sloping bog–forest uplands of the North Coast Forest District, British Columbia, based on a three-component isotope hydrograph-separation analysis conducted in July 1998. At peak discharge during a mid-summer rainfall event, new water contributions accounted for only 12% of streamflow, whereas shallow groundwater accounted for 85% of streamflow and bog groundwater and deep hillslope groundwater accounted for the remaining 3% of streamflow. Mean residence time of water is estimated to be about 2 months, and soil storage capacity is roughly 400 mm based on the analysis of the baseflow discharge and isotopic response. Systematic seasonal shifts in deuterium excess of rainfall in the Prince Rupert area are shown to be useful for labelling shallow and deep groundwaters based on their residence time signatures. The potential for using dissolved organic carbon and deuterium excess as hydrological tracers is also discussed. Copyright © 2000 John Wiley & Sons, Ltd.

KEY WORDS stable isotopes; runoff; wetland; bog; hydrograph separation; deuterium; oxygen-18

INTRODUCTION

Isotope hydrograph separation techniques, in conjunction with hydrometric measurements, have been widely applied to characterize runoff generation mechanisms, for delineating flow pathways, and for estimating water storage capacity (Harris *et al.*, 1995). These factors are known to vary widely geographically, but everywhere are important for understanding water balance and geochemical processes that play an important role in watershed ecosystems. This study, which describes a hydrograph separation analysis conducted within a catchment near Prince Rupert British Columbia, is motivated by the need to identify potential impacts of harvesting on catchment hydrology and stream chemistry in a bog–forest complex.

Wetlands, including sloping bogs, bog forests, bog woodlands and fens account for 51–75% of landcover in the Prince Rupert area of coastal northern British Columbia, an area characterized by rugged landscape, shallow bedrock, high rainfall and low evapotranspiration (National Wetland Working Group, 1997). Residual landcover in what has been referred to as the bog–forest complex consists largely of interspersed low-productivity, open and scrubby stands of western red cedar, cyprus and hemlock. Until recently, these old-growth conifer stands have been considered largely inoperable for clear-cut harvesting owing to low timber volumes. Increasing economic pressures, however, including job creation and waning timber supplies in British Columbia, have prompted the provincial government to consider both the benefits and ecological consequences of harvesting these less productive forests. From a sustainability perspective, specific concerns are that timber regeneration rates may be limited by the extensive occurrence of thick peat deposits and

* Correspondence to: J. J. Gibson, Department of Geography and Wetlands Research Centre, University of Waterloo, Waterloo, ON, N2L 3G1.

Received 20 July 1999
Accepted 18 February 2000

possibly by enhanced rates of peat paludification in harvested areas, or that successful regeneration may require extensive silviculture (Kayahara and Klinka, 1997).

To develop an initial understanding of the ecological processes, including hydrology, geochemistry and peat development, a multidisciplinary study was initiated in 1996 focusing on pre-harvesting conditions at two sites in the Prince Rupert area. In this study, the objective is to understand the exchanges of water between atmosphere, peat and mineral substrate, and surface water outflow. To this end, a three-component hydrograph separation is used to partition event water and two distinct groundwater sources to streamflow during a mid-summer rain event.

Study site

The study was conducted in a 0·33 km^2 watershed on Smith Island, situated 20 km south-east of Prince Rupert and close to the mouth of the Skeena River (Figure 1). The site was selected based on its representativeness of local forest types and for ease of accessibility by boat from nearby Port Edward. Mean annual temperature at Prince Rupert is 6·9°C and mean annual precipitation is 2551 mm (Environment Canada, 1998). Elevation in the watershed ranges from sea level at the outlet (stream gauge, Figure 1) to 396 m near the basin headwaters. Vegetation consists mainly of old-growth forests of the very wet hypermaritime Coastal Western Hemlock zone. There is no recorded history or evidence of fire or harvesting in the catchment. Low productivity stands dominate the watershed (Figure 1), with lesser amounts of more productive forests on steeper slopes, and bogs, fens and transitional bog–forests established in local depressions and in gentle to moderately sloping areas. Poor soil drainage and poor nutrient availability are limiting factors in forest productivity for the region (Banner *et al.*, 1987). As a result, distribution of forest vegetation varies with topography, geology, and the type and frequency of disturbance (Prescott and Weetman, 1994). Bedrock consists of variably fractured plutonic rocks, mainly quartz diorite and granodiorite, and metamorphic rocks, mainly gneiss and schist (Hutchinson, 1982). Although the region was glaciated extensively, glacial deposits are rare in upland areas typical of the watershed. In most areas, a thin mantle of overburden is present (0·5 to 1·5 m thick), consisting of peat, lesser regolith, and minor mineral soils. Organic surficial materials, in the form of forest humus horizons, are observed throughout forested areas and can exceed 40 cm in thickness in upland areas and 70 cm on moderate slopes (Kayahara and Klinka, 1997). Organic deposits in bogs and fens may be up to several metres thick.

Water tables generally were observed to be shallowest in bog areas and deepest on productive slopes. Saturated hydraulic conductivity determined by bail tests ranged from 10^{-4} to 10^{-7} cm/s. Weak downward hydraulic gradients were also observed in hillslope areas and upward gradients were observed near localized seeps and tributary channels. From basic physical monitoring and observation it was found that groundwater flow pathways are typically fairly short, with seep flow contributing most groundwater to streamflow via channelized pathways. Depression storage is commonly observed even during dry periods, but its occurrence during these times is largely restricted to the bog and bog–forest zones. During dry periods, depression storage is encountered on forested hillslopes only for brief intervals during peak runoff. Depression storage occurs throughout the bog–forest complex during wetter periods in autumn and winter.

Methods

Water table wells and shallow piezometers were installed along a transect spanning representative portions of the lower hillslope and lowermost bog (Figure 1). Precipitation was measured using both manual and tipping bucket rain gauges located in open areas near the mouth (3 m a.s.l) and on the bog (45 m a.s.l), respectively. Three additional precipitation stations were maintained at sites ranging in elevation from 5 m to 166 m situated up to 20 km from the site in similar coastal terrain. Throughfall was measured by the method of Spittlehouse (1996) using eavestrough collectors with a combination of tipping bucket and manual rain gauges. Water table response was also recorded on the forested hillslope and on the bog using automated recorders (Remote Data Systems Model WL40^{TM}). Streamflow discharge was determined to within about $\pm$15% using a stage–discharge relationship developed through manual gauging with a portable current

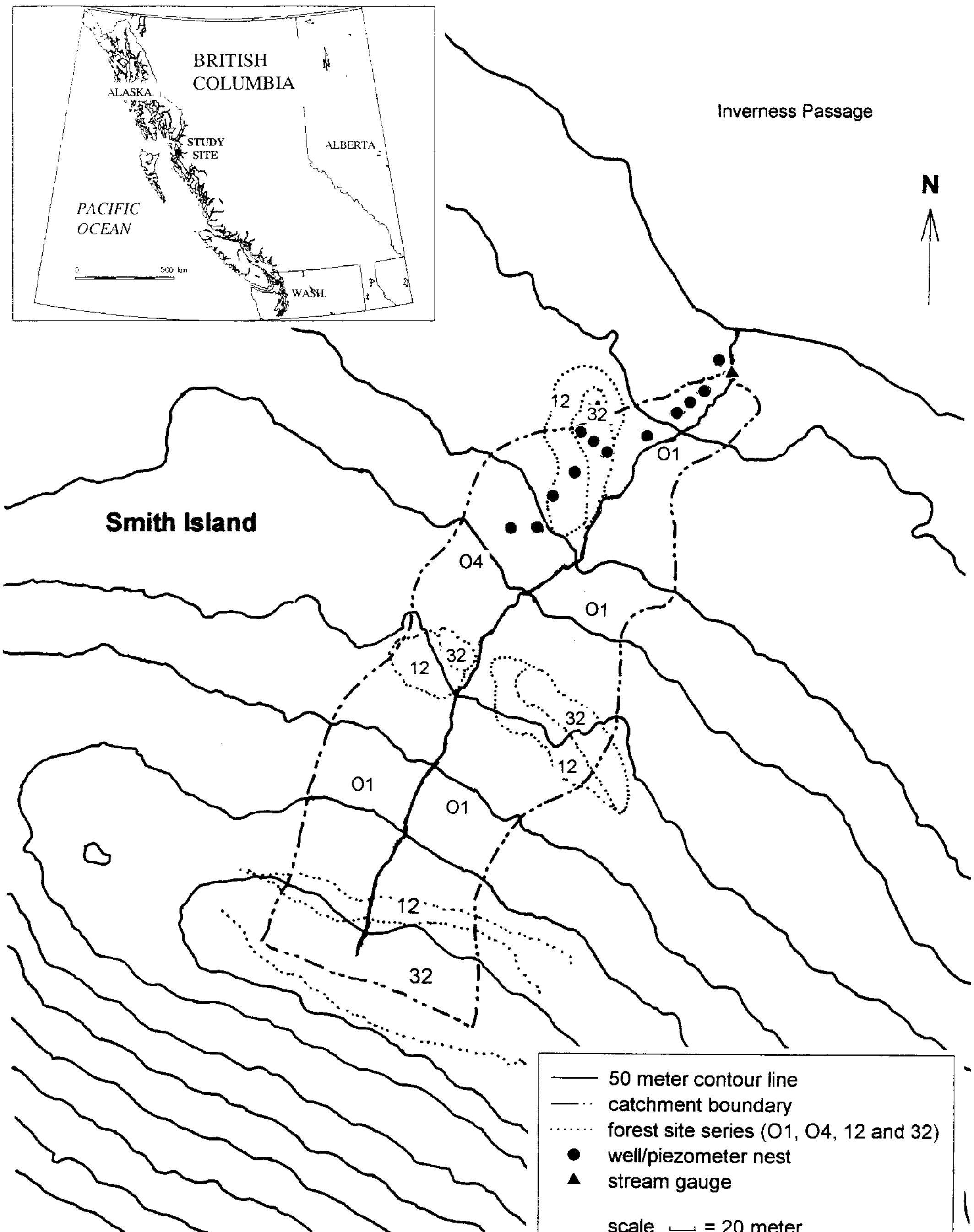

Figure 1. Study site near Prince Rupert, British Columbia, showing location of instrumentation and forest cover types. Note that 01 is low-productivity forest, 04 is high-productivity forest, 12 is bog woodland, and 32 is bog/fen

meter, and stage records based on an atmospherically vented pressure transducer linked to a data logger. The streamflow station (Figure 1) was located above the zone of tidal influence. Standard meteorological measurements such as air temperature, relative humidity, soil temperature and net radiation were installed later in the summer on the lower bog.

Thirty millilitre (1 oz) water samples were collected and returned for standard determination of $^{18}O/^{16}O$ and $^{2}H/^{1}H$ ratios by mass spectrometry at the Environmental Isotope Laboratory, University of Waterloo and results are reported according to the guidelines of Coplen (1996). Based on assessment of laboratory and blind repeats, analytical uncertainty is estimated to be better than $\pm 0{\cdot}1$‰ for $\delta^{18}O$ and ± 2‰ for $\delta^{2}H$.

Water samples for DOC analysis were field filtered (0·45 um), placed in 10-ml rubber-stoppered glass vials, preserved using dilute SO_4, and refrigerated at 4°C until analysed. A syringe was placed in the rubber stopper when capping to minimize trapped air bubbles. Analysis of DOC was by high-temperature combustion at the University of Waterloo. Analytical uncertainty is estimated at $\pm 0{\cdot}5$ mg/l.

A Sigma automatic water sampler was used to collect water samples at the streamflow gauging site during periods when site accessibility was impractical. Each day the autosampler was generally set to collect eight samples at 3-h intervals, although many samples were discarded routinely, except during storm events. Manual samples were used whenever possible to eliminate potential storage effects.

Mass balance theory

Mass balance equations are presented which describe the relative contributions of various water sources to streamflow under a simple batch-mixing model with conservative tracers. More realistic but more complex open-system models have been developed (i.e. Harris *et al.*, 1995) but are not warranted in the present application owing to lack of detailed information on physical and isotopic changes occurring in the source reservoirs. The following model can be applied to separate the instantaneous streamflow discharge into its source components. It also can be applied in a stepwise manner to simulate the effect of temporal changes in source reservoirs and streamflow as they evolve by mixing and interaction with rainfall, surface water or groundwater sources during the course of a high-runoff event.

For a three-component system, the instantaneous streamflow discharge Q is equal to the sum of the contributions from the assumed streamflow sources (x_1, x_2, x_3)

$$x_1 + x_2 + x_3 = Q \tag{1}$$

If the isotopic composition of the water sources is also known or can be estimated, then additional tracer balances can be constructed. In the case of $\delta^{18}O$ and $\delta^{2}H$, which are mass conservative, the mass balance equations are

$$x_1\delta_1^{18} + x_2\delta_2^{18} + x_3\delta_3^{18} = Q\delta_Q^{18} \tag{2}$$

$$x_1\delta_1^{2} + x_2\delta_2^{2} + x_3\delta_3^{2} = Q\delta_Q^{2} \tag{3}$$

where δ_1^{18}, δ_2^{18} and δ_3^{18} are the $\delta^{18}O$ of water sources x_1, x_2 and x_3, and $\delta^2{}_1$, $\delta^2{}_2$ and $\delta^2{}_3$ are the δ^2H of water sources x_1, x_2 and x_3, respectively.

Solving the system of Equations (1) through to (3) for the fractional contribution of the first component of the total streamflow (x_1/Q) then yields

$$\frac{x_1}{Q} = \frac{[(\delta_Q^{18} - \delta_3^{18}) - (\delta_Q^{2} - \delta_3^{2})(\delta_2^{18} - \delta_3^{18})/(\delta_2^{2} - \delta_3^{2})]}{[(\delta_1^{18} - \delta_3^{18}) - (\delta_1^{2} - \delta_3^{2})(\delta_2^{18} - \delta_3^{18})/(\delta_2^{2} - \delta_3^{2})]} \tag{4}$$

It should be noted that contributions from x_1/Q, together with x_2/Q and x_3/Q, which can be evaluated in an analogous way, add up to unity as constrained by Equation (1). A unique solution to Equation (4) also requires that x_1, x_2 and x_3 are not collinear in δ^{18}O versus δ^2H space.

If it is assumed that $\delta_3^{18} = \delta_2^{18}$ and $\delta_2^3 = \delta_2^2$, then Equation (4) reduces to the commonly applied two-point mixing scenario (for δ^{18}O)

$$\frac{x_1}{Q} = \frac{(\delta_Q^{18} - \delta_2^{18})}{(\delta_1^{18} - \delta_2^{18})} \tag{5}$$

For the purposes of this application, and based on the isotopic distinction between different water sources at the study site, the components selected are: (i) event water, (ii) bog/deep hillslope groundwater, and (iii) shallow hillslope groundwater. The rationale for this source-water partitioning scheme is justified later on in the paper.

Deuterium excess

Herein, the *d*-excess parameter, defined by Dansgaard (1964), is used as an index of departure from the Meteoric Water Line (MWL, $\delta^2\text{H} = 8\delta^{18}\text{O} + 10$) of Craig (1961). The *d*-excess parameter is defined as

$$d = \delta^2\text{H} - 8\delta^{18}\text{O}(‰) \tag{6}$$

where δ^2H and δ^{18}O refer to the hydrogen and oxygen isotopic composition of the precipitation water, respectively and 8 is the slope of MWL. (Note that *d*-excess of the MWL is 10‰.) The *d*-excess value is fixed by the air mass origin and air–sea interaction processes, as described by Craig and Gordon (1965) and Merlivat and Jouzel (1979), where increased *d*-excess in precipitation generally reflects enhanced moisture recycling during transport, and lower *d*-excess reflects subdued moisture recycling (Gat *et al*., 1994). The *d*-excess value of groundwater may be altered from the original precipitation source as a result of evaporation in recharge areas, which may cause evaporative enrichment of residual water (Allison *et al*., 1983). The *d*-excess value is not affected by transpiration, which returns groundwater essentially unfractionated to the atmosphere (Gat *et al*., 1994).

RESULTS AND DISCUSSION

Characteristics of rainfall and throughfall sampled during the precipitation event that occurred on 16 July 1998, in comparison with precipitation collected during July 1998, are given in Table I and Figure 2. The physical and isotopic response of the stream and selected reservoirs to the rain event on 16 July is summarized in Figure 2 and in Table II. The DOC concentrations are also shown. A more detailed description of the individual water types is presented below.

Rainfall and throughfall

Daily rainfall and throughfall in the study basin were recorded and collected throughout July 1998 in conjunction with monitoring of groundwater wells, piezometers, seeps and streamflow. A supplementary rain collection station was located at the North Pacific Cannery, situated less than 1 km from the study basin (Cannery, Table I). Subsequent isotopic analysis of rain samples revealed a distinctly labelled 30-mm rain event, which occurred on 16 July 1998 (Day 197) between 11:00 and 23:00 PDT (Figure 2). This event was the largest single rainfall episode in July 1998, but is not considered an extreme event in that it accounted for only 1·2% of the mean annual precipitation recorded at Prince Rupert. The isotopic composition of the rain event measured at the beach site and cannery site was found to differ by less than 4 mm depth and 0·9‰ in δ^{18}O and 3·2‰ in δ^2H, suggesting subdued spatial isotopic variations in precipitation during the event.

Concurrent sampling of rainfall and throughfall was conducted for three separate time intervals during the event, over the periods of 11:00–14:00, 14:00–18:50, and 18:50–23:00. Rain and throughfall over these intervals was found to differ by 0·9‰, 0·9‰ and 2·9‰ in $\delta^{18}O$, respectively, with a weak systematic increase in the ratio of heavy isotopes in rainfall versus througfall during the course of the storm. Similar trends were noted for δ^2H (storm trend, Figure 3a and b). Such minor differences in the isotopic composition of rainfall and throughfall are attributed to canopy effects such as storage, evaporation and rate of flushing of canopy water (Gat, 1996), and also to spatial isotopic variations of precipitation input at the throughfall and rainfall collection sites. The overall relationship between rain and throughfall is demonstrated more clearly when rain and throughfall data are compared over longer time periods. In general, it is found that the isotopic composition of rainfall and throughfall are similar, and are not statistically different from the 1:1 relationship (Figure 3a and b).

Rain and throughfall samples were also collected during a subsequent field visit in late October to early December 1998. On plots of $\delta^{18}O$ versus δ^2H (Figure 4a and b), individual rain events are shown to plot close to the MWL of Craig (1961). Waters sampled during October–December 1998 are distinguished from samples collected during July 1998 by a higher *d*-excess (+ 7·98 versus − 3·78, respectively) with slopes subparallel to the MWL and a high degree of linear correlation in both cases ($r^2 = 0.942$ and $r^2 = 0.997$). The isotopic composition of precipitation collected during the wet season (October–December) was also found to have a narrower range of $\delta^{18}O$ and δ^2H than precipitation collected during the dry season (July) (see Figure 4). Similar seasonal shifts in *d*-excess were measured in monthly weighted precipitation at Victoria, British Columbia during 1975–1982, where average *d*-excess for November was $+7.84 \pm 1.46$ and average *d*-excess for July was -1.80 ± 3.48 (Figure 5) (IAEA/WMO, 1998).

The maritime west-coast climate is known to be dominated by prevailing westerlies and receives frequent cyclonic storms involving cool, moist maritime Pacific air masses. The seasonal *d*-excess signal recorded in 1998 precipitation, with higher *d*-excess in winter and lower *d*-excess in summer, probably reflects seasonal shifts in storm trajectories and air mass history in the region. Enhanced *d*-excess has been attributed to increased admixtures of recycled evaporated moisture, or to reduction in evaporation losses from falling raindrops (Gat, 1996), but these effects remain to be confirmed.

The highly depleted isotopic signature of the 16 July storm strongly suggests that either (i) the air mass experienced pronounced rainout prior to reaching the BC coast or (ii) it was derived from an air mass originating in Arctic continental areas. Ongoing research will continue to address these issues.

Table I. Stable isotope and DOC in rainfall and throughfall

	Pre-event					
Category/type	Amount (mm)	n	$\delta^{18}O$ (‰)	δ^2H (‰)	*d*-excess (‰)	DOC (mg/L)
Rainfall:						
July 1998 (pre-event)	33	7	− 9·7 (2·0)	− 78 (18)	− 0·3 (2·6)	6·9[a] (4·5)
July 1998 (event)						
Beach (precip #1)	30	3	− 22·6 (2·6)	− 173 (24)	7·7 (2·8)	1·9[ab]
Cannery (precip #2)	26	4	− 21·7 (2·2)	− 170 (16)	4·1 (1·5)	–
July 1998 (post-event)	16	1	− 11·1	− 87	1·5	3·2[a]
Throughfall:						
July 1998 (pre-event) (tf #1)	14	4	− 10·8 (1·8)	− 88 (15)	− 1·3 (1·8)	8·2[b]
July 1998 (event) (tf #1)	26	3	− 25·1 (0·12)	− 200 (10)	0·8 (0·9)	7·7[b]
July 1998 (post-event) (tf #1)	16	2	− 10·5 (0·11)	− 79 (2·2)	4·3 (1·3)	8·8[b]

[a]Rain-gauge samples probably contaminated by splash-back from nearby deadfall.
[b]Based on single DOC analysis.

Groundwater and surface waters

The isotopic composition of groundwater sampled in wells and piezometers, and surface water sampled from selected water pools is shown in Table II and Figures 6 and 7. Four water types are distinguished including groundwater and depression storage occurring in bog areas, and shallow and deep groundwater occurring in forested hillslope areas. The fundamental characteristics of these water types as measured during pre-event and post-event sampling is described below.

Pre-event bog groundwater (BGW) sampled in wells and piezometers ranging from 0·7 to 2·6 m depth is found to have an isotopic composition similar to that of pre-event streamflow but with a slightly elevated *d*-

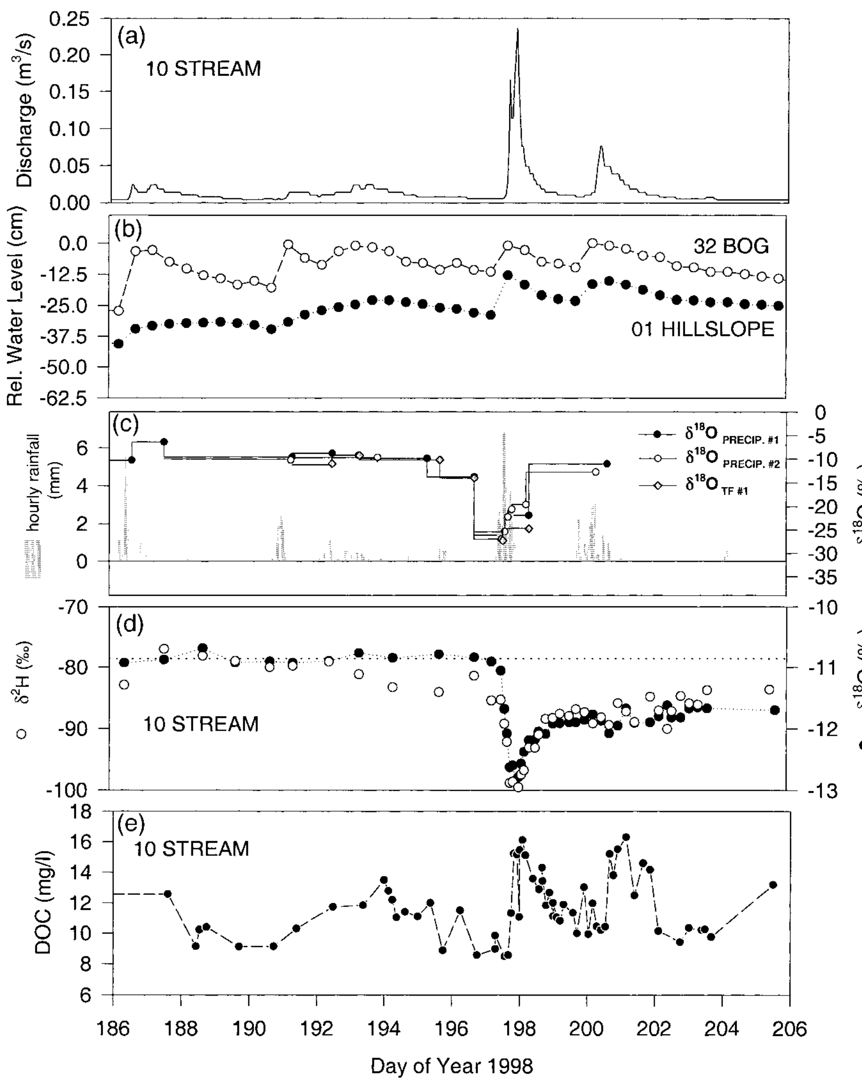

Figure 2. July 1998 time-series of: (a) discharge in main stream (10STREAM); (b) well levels in representative hillslope and bog areas; (c) hourly precipitation, $\delta^{18}O$ of precipitation and throughfall (time of sampling denoted by data points and intervals denoted by stepped lines); (d) $\delta^{18}O$ and $\delta^{2}H$ in streamflow; (e) DOC in streamflow. Note that precip #1 is beach rainfall collector, precip #2 is cannery rainfall collector and tf #1 is throughfall collector (see also Table I).

Table II. Stable isotope and DOC composition of waters by type

	Pre-event					Post-event				
Category/type	*n*	$\delta^{18}O$ (‰)	$\delta^{2}H$ (‰)	*d*-excess (‰)	DOC (mg/l)	*n*	$\delta^{18}O$ (‰)	$\delta^{2}H$ (‰)	*d*-excess (‰)	DOC (mg/l)
Bog water:										
groundwater BGW	12	– 10·8 (0·4)	– 76 (3)	10·0 (2·0)	15·0 (10·3)	5[a]	– 10·9 (0·2)	– 79 (1)	7·8 (2·1)	–
depression storage BDS	6	– 9·5 (2·0)	– 73 (11)	3·25 (6·5)	–	4[b]	– 11·6 (0·3)	– 90 (2)	3·4 (2·2)	10·8 (2·3)
Forest groundwater:										
deep DGW	4	– 11·4 (0·3)	– 81 (2·1)	10·4 (1·6)	6·6 (1·9)	2[a]	– 10·8 (0·1)	– 78 (0·3)	9·0 (0·3)	–
shallow SGW	6	– 11·3 (0·2)	– 87 (1)	3·35 (0·9)	24·0 (18)	3[a]	– 10·6 (0·3)	– 78 (1)	6·4 (1·4)	–
Channelized flows:										
seep flow	2	– 10·5 (0·1)	– 79 (2)	4·3 (1·3)	13·5 (6·1)	4[b]	– 11·7 (0·08)	– 87 (4)	6·2 (4·2)	11·4 (4·2)
streamflow	12	– 10·9 (0·1)	– 81 (3)	5·9 (3·0)	10·1 (1·4)	4[b]	– 11·7 (0·02)	– 84 (3)	9·3 (2·6)	10·9 (1·6)

[a]Denotes samples collected in October/November 1998 and May 1999.
[b]Denotes samples collected in late-July 1998.

excess, and lying closer to the MWL (see Table II and Figure 6). Pre-event bog depression storage (BDS) sampled at various locations along flow pathway trajectories has an isotopic composition indicative in most cases of bog groundwater exposed to evaporation. Individual pools lie along a local evaporation line with a slope of about 6 in $\delta^{18}O$ versus $\delta^{2}H$ space (Figure 6), and are characterized by varying degrees of evaporative isotopic enrichment depending on their residence time and flushing rates. The slope of the evaporative enrichment trend suggests evaporation at moderate to high relative humidity (60–80%), which is typical during summer dry periods. Two exceptions include a water pool that was found to have a pre-event isotopic signature similar to that of July precipitation, and a water pool that evidently contained substantial amounts of deep groundwater. Sampling and analysis of post-event bog depression storage (BDS) revealed that the surface pools had probably been flushed and homogenized, which resulted in final isotopic compositions similar to recent precipitation (Figure 6).

Pre-event groundwaters sampled in forested hillslope areas are classified as shallow (SGW) and deep groundwater (DGW) (Table II). Shallow groundwater is characterized by occurrence within forest peat at depths of less than 0·6 m, and isotopic similarity to summer precipitation, suggesting relatively short water residence times of less than one year. In two cases, shallow groundwater signatures were also detected at the bedrock contact at depths of 1·2 m and 1·8 m, presumably indicating rapid transport of water to depth by soil macropores. (Note that this water is classified as shallow groundwater for the purposes of the hydrograph separation.) Deep groundwater is named as such owing to its occurrence in forest peat at generally greater depths, ranging from 0·7 to 1·3 m, and its isotopic signature, which is more typical of annual precipitation, suggesting longer residence times. Based on pre-event isotopic composition, these waters are distinguished by a systematic offset in *d*-excess, where shallow groundwater is characterized by $d = 3.4 \pm 0.9‰$ and deep hillslope groundwater and bog groundwater are characterized by $d = 10.0 \pm 2.0‰$ (Figure 6b, inset 2). Deep groundwater has a similar isotopic signature to bog groundwater, although the latter is slightly enriched in $\delta^{18}O$ and $\delta^{2}H$ owing to evaporative effects or, possibly, to differences in water residence times and hence isotopic weighting in these reservoirs. Comparison of the isotopic composition of

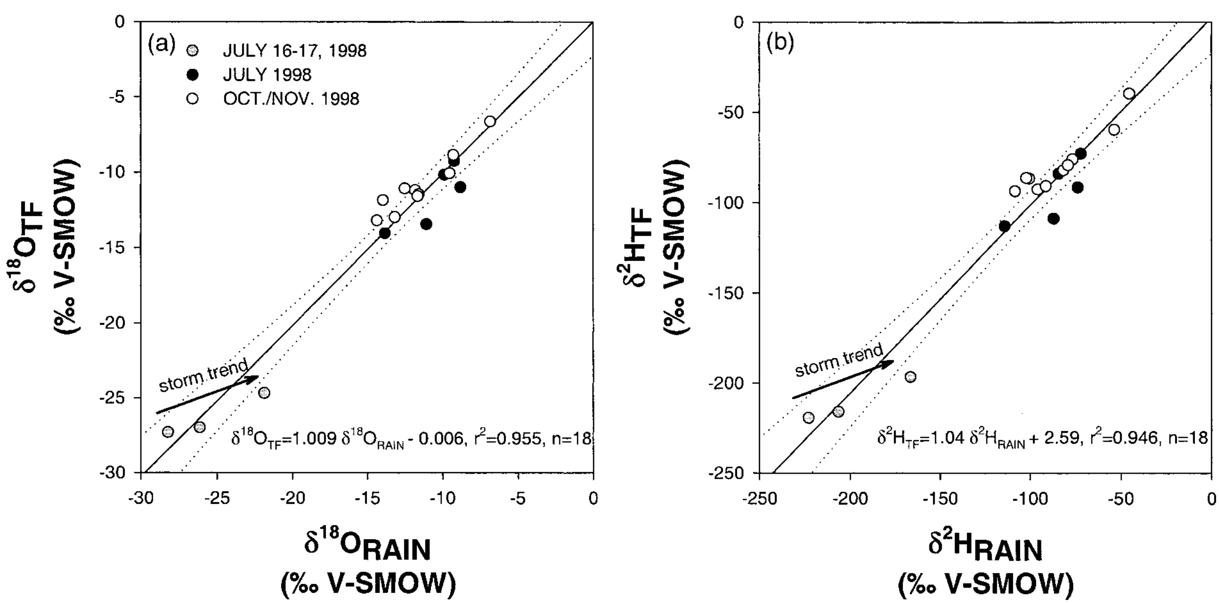

Figure 3. Crossplots of the isotopic composition of rain and throughfall: (a) for $\delta^{18}O$ and (b) for $\delta^{2}H$. Sampling periods are denoted by separate symbols as shown. Note that overall correlations obtained by linear regression using all data are not significantly different than the 1:1 trend. Note that samples were collected during different field campaigns as indicated

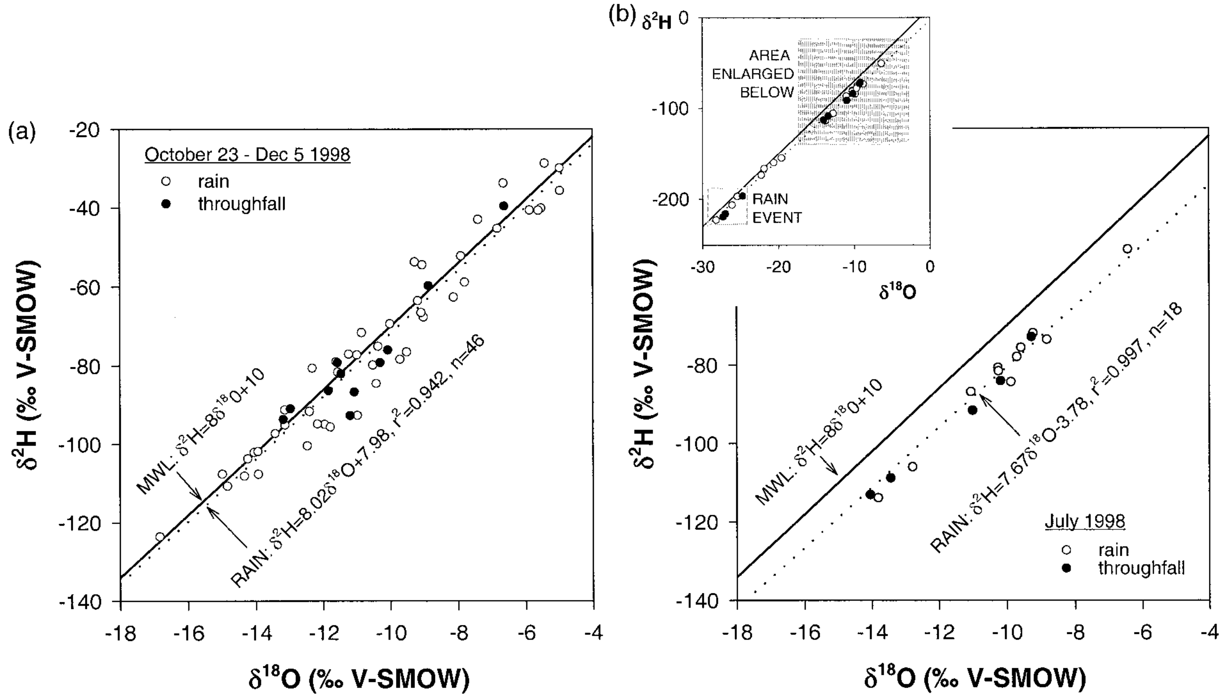

Figure 4. Plots of $\delta^{18}O$ versus δ^2H for rain and throughfall: (a) October–December 1998 and (b) July 1998. Note that throughfall data are excluded from the regression analysis. Inset shows plot of $\delta^{18}O$ versus δ^2H with axes extended to illustrate the pronounced isotopic separation between the rain event and other July precipitation. Note that rainfall samples plot along a slope close to the MWL in both cases, but with systematic offset in the *d*-excess of precipitation from the wet season (October–December 1998) to the dry season (July 98)

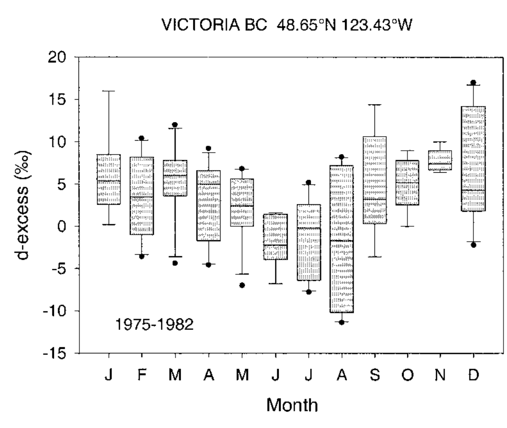

Figure 5. Box-and-whiskers plot of *d*-excess in monthly precipitation sampled at Victoria, British Columbia during 1975–1982. Note that lines within the boxes denote median values, top and bottom of boxes denote 25th and 75th percentiles of year-to-year values, and whiskers denote 10th and 90th percentiles of year-to-year values. Outliers are also shown. Note also the seasonal shift in *d*-excess with minimum values generally observed in mid-summer (June, July and August). Data obtained from IAEA/WMO (1998)

pre-event and post-event groundwaters reveals that bog groundwater and deep hillslope groundwater are less variable than shallow groundwater and depression storage (Table III, see also Figures 6 and 7).

Overall, the distinctive isotopic signals in groundwater and surface water are interpreted to be the result of the combined effects of seasonal variations in the isotopic signature of precipitation input, variations in water residence times in the various terrain units, and minor evaporative enrichment. Stability of bog isotopic signatures is expected considering the low hydraulic conductivity of blanket peat in the bogs, low hydraulic gradients, and presence of relatively few macropores. Bog groundwater and deep hillslope groundwater, with relatively long residence times, retain the isotopic signal of precipitation weighted over periods of several years or longer, whereas shallow groundwater with a shorter residence time retains the isotopic signal of precipitation falling during the preceding month or two.

Owing to the seasonal cycle of *d*-excess, the net result is a hydrological system that is labelled isotopically according to water residence times. This idea is supported by the observation that bog water, as with mean annual precipitation, lies close to the MWL and October to December 1998 precipitation trends (2, Figure 6a), whereas shallow groundwater lies closer to the precipitation trend for July 1998 (1, Figure 6a).

It is significant to note that identifying the cause of the distinctive isotopic signals in groundwater was not possible without the combined use of $\delta^{18}O$ and δ^2H, which also permitted characterization of the *d*-excess parameter. As shown in Figure 7, isotopic gradients across the bog–forest transition were gradual, and peaks in both tracers in the bog areas (when observed alone) may have been mistaken for evaporative enrichment effects. Evaporation alone, however, cannot explain these differences because evaporative isotopic enrichment, even at high humidity, will not produce the observed increase in *d*-excess in bog groundwater

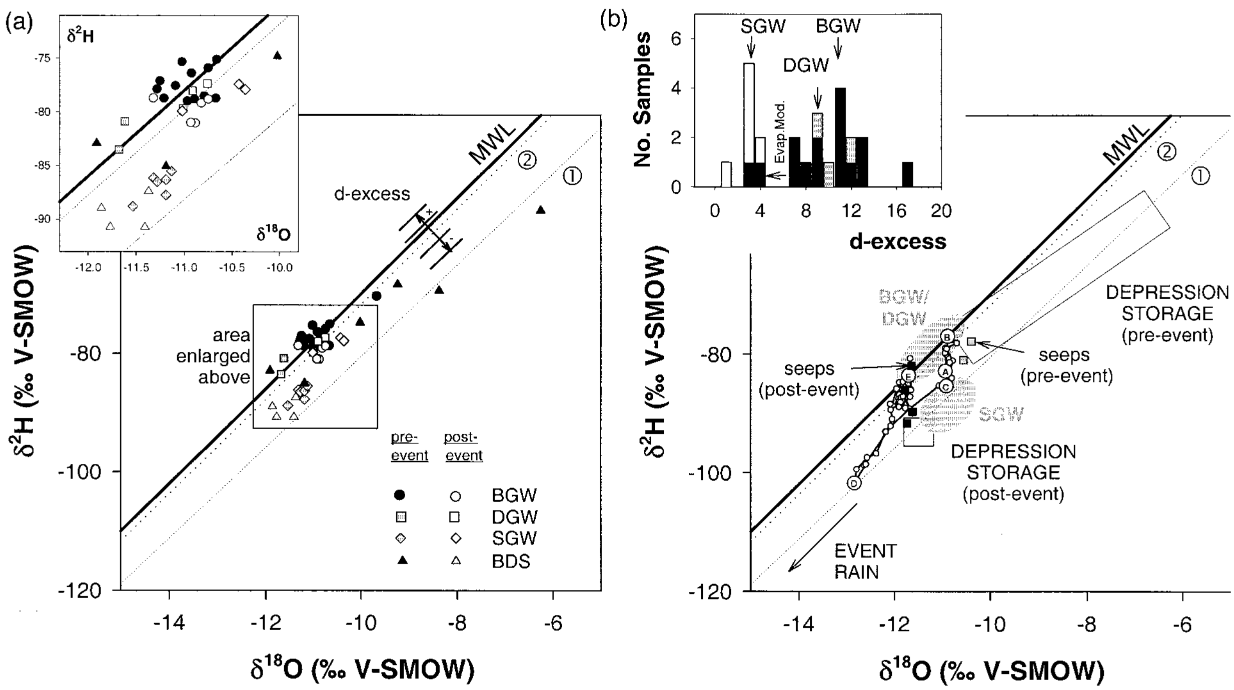

Figure 6. Plots of $\delta^{18}O$ versus δ^2H showing (a) groundwaters and surface waters including bog groundwater (BGW), deep hillslope groundwater (DGW), shallow groundwater (SGW) and bog depression storage (BDS) sampled during May and late July 1998 (pre-event) and late July 1998, October/November 1998 and May 1999 (post-event), and (b) the evolution of isotopic composition of bog depression storage (BDS), seeps and streamflow during July 1998. Note that lines labelled 1 and 2 are the precipitation trends for July 1998 and October to December 1998 from Figure 4. Inset shows frequency distribution of *d*-excess in groundwater illustrating differences between SGW (open bars), DGW (grey bars), and BGW (solid bars). See text for discussion

(BGW) as compared with shallow hillslope groundwater (SGW) (Table II). Evaporated waters normally will plot along lines with slope of 4 to 8 in $\delta^{18}O$–$\delta^{2}H$ space, and characteristically attain lower *d*-excess values as evaporation progresses. From theoretical considerations, the upper limit on the evaporative enrichment slope of 8 occurs at a relative humidity of 100%, and is imposed by the ratio of the equilibrium fractionation factors (ε^*) of the isotopic species, i.e. $\varepsilon_2^*/\varepsilon_{18}^* \approx 8$, which corresponds to the slope of the MWL (see Gat, 1996). The offset between SGW and BGW therefore is not attributable to evaporative effects.

Seeps and streamflow

Channelized flows, including flow in the main stream and tributary seep channels, were sampled before and after the 16 July rain event.

Seep flow and streamflow had isotopic signatures intermediate between DGW/BGW, SGW and BDS, reflecting a mixture of these components (Figure 6b). Seeps and streamflow were found to be isotopically similar both before and after the rain event, although only the streamflow was sampled regularly throughout its duration (Figure 6b). Isotopic similarity between seeps and streamflow is consistent with basic observations that seeps are a dominant pathway of water movement. The progression of streamflow isotopic composition throughout the rain event is depicted in Figure 6b, the temporal streamflow isotopic trend being sequentially labelled A through to E, which correspond to:

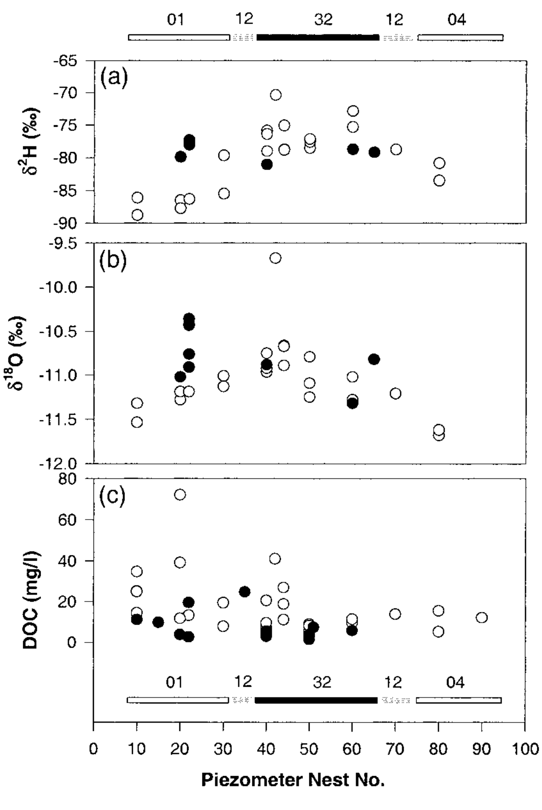

Figure 7. Gradients in $\delta^{18}O$, $\delta^{2}H$ and dissolved organic carbon (DOC) along the main well transect across representative vegetation zones. Note that 01 is low-productivity forest, 04 is high-productivity forest, 12 is bog woodland, and 32 is bog/fen. Open circles indicate pre-event samples and closed circles indicate post-event samples. See text for discussion

Table III. Summary of isotopic variability in surface water and groundwater reservoirs

		$\delta^{18}O$ (‰)				$\delta^{2}H$ (‰)				d-excess (‰)			
Category/type	n	Maximum	Minimum	$\Delta\delta^{18}O$	1 SD	Maximum	Minimum	$\Delta\delta^{2}H$	1 SD	Maximum	Minimum	Δd	1 SD
Bog groundwater BGW	16[a]	−10·7	−11·3	0·7	0·2	−81	−73	8·1	2	12·9	6·0	6·9	2·3
Deep groundwater DGW	6	−10·8	−11·6	0·9	0·4	−84	−77	6·2	2	12·1	8·4	3·7	1·3
Shallow groundwater SGW	9	−10·4	−11·5	1·2	0·4	−89	−77	11·4	4	8·3	1·8	6·5	1·8
Depression storage BDS	10	−6·3	−11·9	5·7	1·8	−56	−91	35	11	12·3	−6·0	18·3	4·8

[a]Excludes one anomalous bog groundwater sample that has been significantly modified by evaporative enrichment.

(A) early July streamflow comprising pre-event rain, shallow groundwater (SGW) and deep/bog groundwater (DGW/BGW);
(B) pre-event streamflow dominated by deep/bog groundwater (DGW/BGW);
(C) maximum shallow groundwater (SGW) contributions at the time of peak discharge;
(D) maximum event water contributions;
(E) post-event streamflow dominated by deep/bog groundwater (DGW/BGW).

Post-event streamflow and seep flow are shown to be depleted in both $\delta^{18}O$ and $\delta^{2}H$ relative to pre-event flows owing to the residual presence of event water (Figure 6b).

Event streamflow

The rain event that occurred on 16 July 1998 between 11:00 and 23:00 PDT (centroid at 17:00) produced a water table response in bog and hillslope wells, in streamflow discharge, and in streamflow isotopic composition and DOC content (Figure 2). Streamflow peaked at 237×10^{-3} m^3/s within 8 h of the storm centroid (and within 2 h of cessation of rainfall) and gradually receded to a baseflow of 5.5×10^{-3} m^3/s within 5·4 days (Table IV). Overall, the response of the system can be considered flashy. Water tables in a representative hillslope area ranged from about 0·25 to 0·40 m depth before the event to about 0·13 m depth during peak flow. Similarly, the water table in the bog ranged from about 0·25 to 0·05 m depth before the event and rose near surface or above surface during peak flow. Abundant surface flow in streamlets connecting depression storage pools was also observed on the bog and to a lesser extent in local channels or rills in forested hillslope areas. Water table recession times were similar to those observed for streamflow (Figure 2). Cumulative streamflow discharge from peak flow to the end of the observation period (day 206) is estimated at about 14700 m^3 or roughly 150% of event rainfall. Note that for the period 3 July to 24 July 1998 (day 184–205), the opposite was true, i.e. rainfall was equal to 150% of runoff.

Around the time of peak event runoff on 17 July (day 198) at 02:00, the isotopic composition of streamflow reached a local minimum, depleted by 2‰ in $\delta^{18}O$ and 20‰ in $\delta^{2}H$ compared with pre-event streamflow, evidently as a result of the presence of event water. The isotopic recession to baseflow continued for at least 8 days, indicating gradually diminishing contributions of event water, and was extended by at least several days relative to the discharge recession. This lag effect, which has been observed in other high-rainfall catchments (Bonell *et al.*, 1998) has been attributed to isotopic modification of groundwater by event water, indicative of systems where surface and subsurface hydrology are strongly linked. In the present setting, this connection is assured by the universal presence of peat, which implies a shallow water table. Detailed temporal groundwater sampling was not conducted during the event to verify this hypothesis, although considerable retention of event water is evident based on the slow tracer recovery (see below).

Three-component hydrograph separation

Event rainfall and baseflow in the stream differed by 11·7‰ in $\delta^{18}O$ and 92‰ in $\delta^{2}H$, roughly 100 and 50 times the analytical uncertainty of each tracer, respectively. Approximately 9900 m^3 of this well-labelled water was added to the study basin during the 12-h rain event, providing an excellent natural tracer experiment. Streamflow discharge is partitioned for the duration of this event using Equation (4) to separate total discharge into its component contributions, namely event-water, shallow groundwater and deep/bog groundwater (Table IV). These components are selected based on their distinctive $\delta^{18}O$, $\delta^{2}H$ and *d*-excess signatures, and because they have shown to be distinct and significant streamflow sources in high-rainfall catchments (Bonell *et al.*, 1998). Note that *d*-excess could be equally substituted for either $\delta^{18}O$ or $\delta^{2}H$ in the balance equations, as demonstrated for the case of atmospheric water balance by Gat *et al.* (1994). Constant pre-event values from Table II are taken directly to characterize event and shallow groundwater contributions, whereas mean values of pre-event bog groundwater and deep groundwater are used together to characterize the third component, based on the assumption that bog groundwaters are probably better

Table IV. Streamflow partitioning summary

Interval/ category	Time since event rainfall centroid, day 197 at 17:00	Percentage of specified component in instantaneous streamflow			Instantaneous discharge ($\times 10^{-3}$ m^3/s)			
		Event water	BGW/DGW	SGW	Event water	BGW/DGW	SGW	Streamflow
Pre-event	0	2[a]	44	54	0·2	4·4	5·4	10
Event:								
mean	–	8	35	57	4·4	6·5	33	44
peak discharge	+ 8 h	12	3	85	29·2	7·1	201	237
maximum Q_N/Q_{TOTAL}	+ 9·4 h	13	2	85	15	2·3	97	114
minimum Q_N/Q_{TOTAL}	+ 4·8 days	6[b]	49[b]	45[b]	0·5[b]	3.[b]]	3·6[b]	8·0[b]
low flow	+ 5·4 days	6	56	38	0·3	3·1	2·1	5·5
Post-event	+ 5·4–8 days	7	73	20	0·4	4·2	1·1	5·7

[a]Denotes estimated contributions from rain prior to the 16–17 July event.
[b]Adjusted to account for interference from secondary event.

weighted values of long residence time sources. As a consequence, bog groundwater and deep groundwater flow from hillslopes are combined as a single component.

Temporal trends in computed discharge of individual water components during the event are illustrated in Figure 8. Note that confidence in the separation between event and pre-event groundwater is superior to the separation between shallow versus deep/bog groundwater flow, owing to the extreme isotopic differences between event and pre-event waters. Errors here are roughly 2% for the Q_N/Q_{TOTAL} partition versus 20% for the Q_{SGW}/Q_{DGW} partition, respectively.

Peak discharge in the streams was found to be dominated by shallow groundwater flow from forested hillslopes (85%), with lesser contributions from event water (12%) and deep/bog groundwater sources (3%).

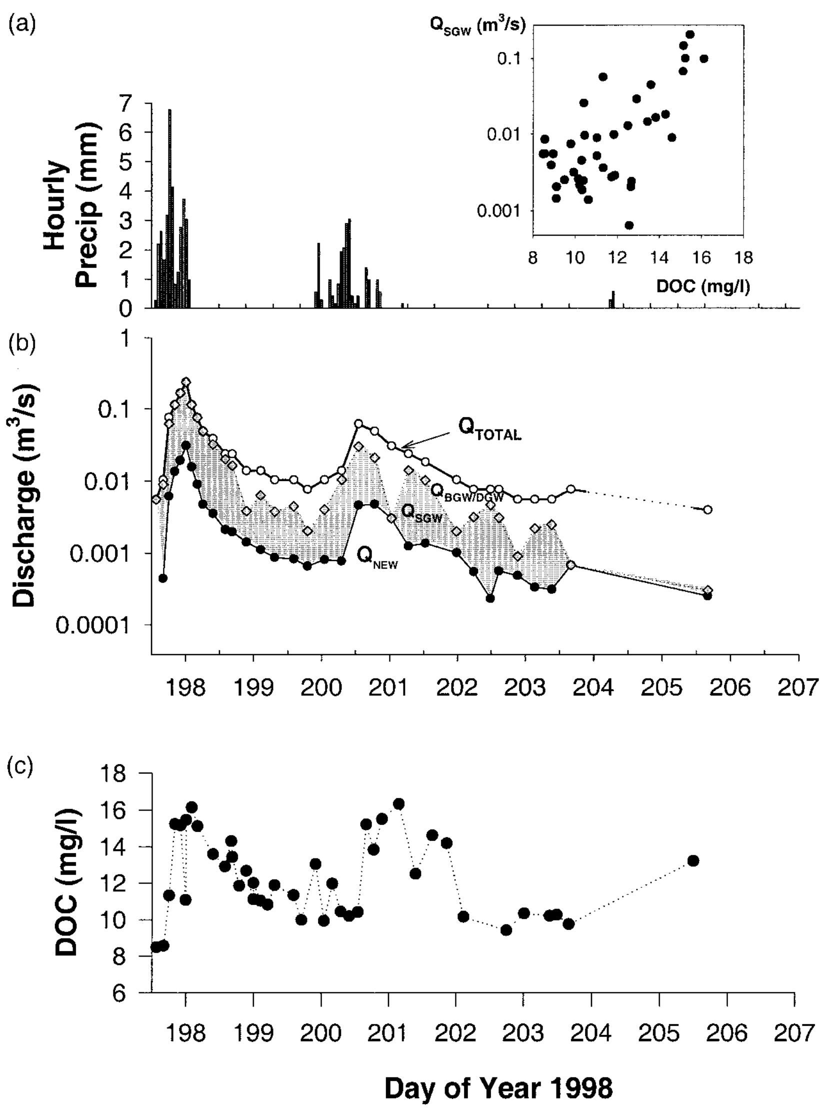

Figure 8. July 1998 time-series of: (a) hourly precipitation; (b) discharge of total streamflow (Q_{TOTAL}) partitioned according to event water (Q_N), shallow hillslope groundwater (Q_{SGW}) and deep groundwater flow (Q_{DGW}); (c) dissolved organic carbon (DOC). Inset is a plot of streamflow DOC versus Q_{SGW} illustrating the positive correlation ($r^2 = 0.44$)

Maximum instantaneous Q_N/Q_{TOTAL} and Q_{SGW}/Q_{TOTAL} of 13% and 85%, respectively, occurred concurrently at 1·4 h after peak discharge, with instantaneous Q_N/Q_{TOTAL} declining to about 6% within 5·4 days. As the recession proceeded, deep groundwater (including bog groundwater) evidently began to contribute more substantial fractions of water to streamflow, although absolute discharge of deep groundwater and bog groundwater was also receding (Table IV).

Such variations in Q_N/Q_{TOTAL} (in the range of *c.* $\sim$0–40%; Buttle, 1994) have been widely observed during rain events in upland forested catchments, although none of these have been systems dominated by organic deposits. In any case, the high proportion of groundwater in the stormflow attests to the importance of subsurface interaction in the basin. Subsurface flow pathways, although short and often terminating in seeps and rills within several metres of the zone of recharge, are nevertheless critical to the rainfall–runoff transition. Presumably, peak event-water contributions are also diminished by the delaying effect of canopy storage resistance, which also may limit direct precipitation to near-stream areas.

Soil storage and water residence times

Cumulative discharge of event water to day 206 is estimated at 1330 m^3 or 13% of the 9900m^3 event input. Based on the assumption that about 20% of the event water is diverted to interception loss (1700 m^3), as determined by comparing precipitation and throughfall records for the summer months, it is estimated that 6900 m^3 of event water was recharged to groundwater reservoirs (including bog storage) in the catchment. From evidence obtained from the isotopic difference between baseflow before and after the event (i.e. a shift of $-0{\cdot}81‰$ in $\delta^{18}O$ and $-3{\cdot}1‰$ in δ^2H), and knowledge of the event isotopic composition and volume of event water, an estimate of the total groundwater storage is obtained by Equation (5) of close to 125000 m^3 or 400 mm over the basin. This is at the upper end of the normal spectrum of soil-water storage capacity commonly used in hydrological models (e.g. Thornthwaite and Mather, 1957) but is a reasonable value compared with preliminary estimates computed from measured soil depth multiplied by porosity. This translates into mean water residence times of approximately 2 months for the integrated basin, although it is acknowledged that residence times locally may range from near zero to decades or longer as in the case of bogs. Overall, the presence of bedrock at shallow depth and the steeply sloping nature of the watershed combine to limit storage capacity in the watershed. Based on estimates of hydraulic conductivity and water residence times it is predicted that average groundwater flow pathways are probably less than about 5 m. This corroborates field observations, which suggest a groundwater system that is fully linked to channelized surface flow in seeps and streams.

Dissolved organic carbon (DOC)

Measured DOC variations in streamflow and contributing sources (Tables I & II and Figure 2) offer further support for the dominance of shallow groundwater flow at the time of peak discharge. Rainfall, collected near ground level during the pre-event period, shows an average DOC concentration of $6{\cdot}9 \pm 4{\cdot}5$ mg/L, which may be slightly elevated above levels in incident precipitation as a result of splashback contamination from deadfalls near the collector. Nevertheless, values obtained for the event and post event conditions (Table I), which are also likely to be affected by splashback contamination from deadfall, are within the expected range for precipitation measured elsewhere (Moore, 1989). Throughfall is characterized by DOC concentrations around 8 mg/L. Bog groundwater (BGW) is characterized by an average DOC value of $15{\cdot}3 \pm 10{\cdot}3$ mg/L (Table II). These are typical values for DOC produced in bogs (e.g. Schiff *et al.*, 1997). Shallow groundwater (SGW) shows significantly higher DOC values than deep groundwater (DGW), averaging 24 ± 18 mg/L and $6{\cdot}6 \pm 1{\cdot}9$ mg/L, respectively; Table II). This pattern probably results from the occurrence and movement of shallow groundwater through the organic-rich surficial deposits on hillslopes. The lower DOC concentration observed in the deep groundwater probably is the result of DOC losses by consumption and absorption during transport as water percolates through the soil (McDowell and Wood, 1984; Moore *et al.*, 1992). The stream under pre-event condition shows DOC concentration in the range of $10{\cdot}1 \pm 1{\cdot}4$ mg/L. These values are higher than data reported for terrestrial forested watersheds (e.g. Hinton *et al.*, 1997) and similar to streams in catchments where swamps and bogs cover a significant part of the watershed (Mulholland, 1981; Schiff *et al.*, 1997). It is postulated that the hillslopes, which are formed by organic-rich soils with a carbon content similar to bogs, are the main sources of DOC to the stream in the study area. This is inferred from the high DOC concentration measured in the hillslope groundwater representing the main vegetation zones (Figure 7).

Significant changes in DOC are observed in the stream during the event (Figure 8). The DOC concentrations are positively correlated with log Q_{SGW} ($r^2 = 0.44$, Figure 8) and are found to double at the time of peakflow versus baseflow, consistent with abundant contributions from DOC-rich sources in shallow hillslope soils, and lesser contributions from DOC-poor rainfall, throughfall, bog groundwater and deep groundwater sources. Significant DOC also may be derived from bog depression storage, which could account for some variability in streamflow compositions, although these reservoirs were not sampled for DOC prior to the event. Hillslope groundwaters were found to have higher DOC concentrations in the dry season than in the wet season, which is indicative of DOC accumulation (less flushing) and/or higher biotic activity (Figure 7). Correlation between log Q_{BGW} and DOC is poor ($r^2 = 0.09$), suggesting that the majority of DOC is not derived from deep hillslope groundwater or from bog groundwater.

Although DOC is not a conservative tracer *per se* it does offer considerable potential in the current setting as a semi-quantitative hydrological tracer. Although further research to achieve a better understanding of DOC-controlling processes is required to assess the suitability of DOC as a tracer of runoff generation processes, this work is warranted because of potential for expanding analysis to include individual events that are not labelled distinctly by either oxygen-18 or deuterium.

Runoff mechanisms

The role of groundwater in the runoff regime of hypermaritime bog–forest complexes of the Prince Rupert region has not been investigated previously. From basic observations we can conclude that water reaching the ground surface passes through the subsurface along short flow pathways that terminate in local rills or seeps. The prevalence of low hydraulic conductivity organic soil promotes shallow water tables and effectively reduces the rate of groundwater movement in deeper organic soils below about 0·5 m depth. This condition appears to limit interaction between bedrock and shallow groundwater, resulting in geochemically dilute waters and runoff. Drainage from the slopes occurs primarily via channelized flow in seepage tracks, often deeply incised, that typically are connected to the main stream channel. Water with the distinct isotopic signature of shallow groundwater flow also has been observed at the bedrock interface, and is attributed to the presence of vertical bypass structures created by buried deadfall and/or root holes, although these have not been widely observed. The groundwater regime within bedrock has not been investigated, but recharge is expected to occur from the overlying organic layers, especially in the bog-filled depressions, owing to the fractured character of the rock mass.

Bonell *et al.* (1998) describe analogous hydrological and isotopic responses in high-rainfall response-dominated tropical forested catchments of New Zealand and Australia with shallow soils ($<$ 3 m) overlying bedrock. At low rainfall intensities ($<$ 250 mm/day), they observed that water generally is routed to streamflow via the soil–groundwater system, which can be predominantly characterized as a first-in-first-out system, i.e. streamflow is dominated by old water. At high rainfall intensities ($>$ 250 mm/day), however, the flow capacity of these pathways is exceeded and alternative pathways involving rapid flow (i.e. rill and seep flow) are invoked, resulting in last-in-first-out behaviour, i.e. streamflow is dominated by new water. They concluded that these steep, flashy hydrological systems with shallow soils (3 m) overlying bedrock are well-represented by an ideal non-linear storage model that is comprised of a shallow, quick flow reservoir coupled to a deep slow flow reservoir (figure 11·19 in Bonell *et al.*, 1998).

This study indicates that a similar conceptual model may apply to temperate rainforests characterized by bog–forest vegetation. Although soil layers are considerably shallower in the present setting, variations in the organic content of soil, and variations in the depth of soils combine to produce considerable variability in water residence times in various terrain units within the watershed. Based on the studies of Bonell *et al.*

(1998) it is probable that high intensity events (not observed in this study) may be characterized by a shift or perhaps a reversal in old and new water contributions. Further physical monitoring and isotope hydrograph separation analysis will be required to refine and improve on this conceptual model of runoff generation.

CONCLUDING COMMENTS

Through application of isotope hydrograph separation, this study has developed a conceptual basis for understanding the hydrology of a complex area. This understanding will be applied to develop and test ecosystem models, and to design better networks to observe impacts resulting from forest harvesting. From these studies it is expected that residence times of groundwater will be affected and changes may occur in the first season following disturbance by harvesting.

It is important to note that measurement of both δ^{18}O and δ^{2}H was required to distinguish bog and hillslope sources, and to characterize the *d*-excess effects. Determination of *d*-excess offers considerable potential to map the residence time distribution of groundwater within the catchment. The concentration of DOC is also a potentially useful tracer of water cycling processes to extend observations beyond those events that are labelled isotopically.

Future research will involve specific issues not addressed in the current paper, including detailed time-series monitoring of the physical, isotopic and geochemical (including DOC) evolution of groundwater during storm events, the orographic effect of precipitation, and geochemical implications. Planned studies will also assess the direct impact of harvesting in the study watershed.

ACKNOWLEDGEMENTS

Funding for this research was provided by a grant from Forest Renewal British Columbia. Special thanks to Richard Elgood and Tony Duggleby for assistance in the laboratory and field respectively. We owe a debt of gratitude to Dr Terry Prowse of the National Water Research Institute, Saskatoon who graciously loaned the autosampler. Isotopic analyses were skillfully performed by staff of the Environmental Isotope Laboratory, University of Waterloo. This manuscript has benefited from the comments of two anonymous reviewers.

REFERENCES

Allison GB, Barnes CJ, Hughes MW. 1983. The distribution of deuterium and ^{18}O in dry soils. *Journal of Hydrology* **64**: 377–397.

Banner A, Pojar J, Kimmins JP. 1987. The bog–forest complex of north-coastal British Columbia. In *Proceedings: Symposium '87 Wetlands/Peatlands*, Edmonton, Alberta, 483–491.

Bonell M, Barnes CJ, Grant CR, Howard A, Burns J. 1998. High rainfall, response-dominated catchments: a comparative study of experiments in tropical northeast Queensland with temperate New Zealand. In *Isotope Tracers in Catchment Hydrology*, Kendall C, McDonnell JJ (eds). Elsevier: New York; 347–390.

Buttle JM. 1994. Isotope hydrograph separations and rapid delivery of pre-event water from drainage basins. *Progress in Physical Geography* **18**: 16–41.

Coplen TB. 1996. New guidelines for reporting stable hydrogen, carbon, and oxygen isotope-ratio data. *Geochimica Cosmochimica Acta* **60**: 3359–3360.

Craig H. 1961. Isotopic variations in meteoric waters. *Science* **133**: 1833–1834.

Craig H, Gordon LI. 1965. Deuterium and oxygen 18 variations in the ocean and marine atmosphere. In *Stable Isotopes in Oceanographic Studies and Paleotemperatures*, Tongiorgi E (ed.). Laboratorie Geologia Nucleare: Pisa; 9–130.

Dansgaard W. 1964. Stable isotopes in precipitation. *Tellus* **16**: 436–468.

Environment Canada. 1998. Canadian Climate Normals 1961–90, Prince Rupert A, British Columbia, *http://www.cmc.doe.ca/climate/normals/BCP017.htm*.

Gat JR. 1996. Oxygen and hydrogen isotopes in the hydrologic cycle. *Annual Reviews in Earth and Planetary Sciences* **24**: 225–262.

Gat JR, Bowser CJ, Kendall C. 1994. The contribution of evaporation from the Great Lakes to the continental atmosphere: estimate based on stable isotope data. *Geophysical Research Letters* **21**: 557–560.

IAEA/WMO. 1998. Global Network for Isotopes in Precipitation. The GNIP Database. Release 2 May 1998. Monthly Data, Victoria Canada, 1975–82. URL: *http://www.iaea.org/programs/ri/gnip/gnipmain.htm*.

Harris DM, McDonnell JJ, Rodhe A. 1995. Hydrograph separation using continuous open system isotope mixing. *Water Resources Research* **31**: 157–171.
Hinton MJ, Schiff SL, English MC. 1997. The significance of storms for the concentration and export of dissolved organic carbon from two Precambrian Shield catchments. *Biogeochemistry* **36**: 67–88.
Hutchinson WW. 1982. Geology of the Prince Rupert–Skeena map area, British Columbia. *Geological Survey of Canada Memoir* **394**: 116 pp .
Kayahara GJ, Klinka K. 1997. The Potential for Managing Nutrient Poor and Low Productivity Yellow Cedar–Hemlock Forests of North Coastal British Columbia: a Problem Analysis. Technical Report, Ministry of Forests: British Columbia; 51 pp.
McDowell WH, Wood T. 1984. Podzolization: soil processes control dissolved organic carbon concentration in stream water. *Soil Science* **137**: 23–32.
Merlivat L, Jouzel J. 1979. Global climatic interpretation of the deuterium–oxygen 18 relationship for precipitation. *Journal of Geophysical Research* **84**: 5029–5033.
Moore TR. 1989. Dynamics of dissolved organic carbon in forested and disturbed catchments Westland, New Zealand. 1. Maimai. *Water Resources Research* **25**: 1321–1330.
Moore TR, de Souza W, Koprivnjak JK. 1992. Controls on the sorption of dissolved organic carbon in soils. *Soil Science* **154**: 121–129.
Mulholland PJ. 1981. Organic carbon flow in a swamp–stream ecosystem. *Ecological Monographs* **51**: 307–322.
National Wetland Working Group. 1997. *The Canadian Wetland Classification System*, 2nd edn, Warner BG, Rubec CDA (eds). Wetland Research Centre Publication: Waterloo, ON; 68 pp.
Prescott CE, Weetman GF (eds). 1994. Salal Cedar Hemlock Integrated Research Program: a Synthesis. The Department of Forest Sciences, Faculty of Forestry, University of British Columbia: Vancouver, British Columbia; 85 pp.
Schiff SL, Aravena R, Trumbore SE, Hinton MJ, Elgood R, Dillon PJ. 1997. Export of DOC from forested catchments on the Precambrian Shield of Central Ontario: Clues from ^{13}C and ^{14}C. *Biogeochemistry* **36**: 43–65.
Spittlehouse DL. 1996. Rainfall interception in young and mature conifer forests in coastal B.C. *Canadian Journal of Soil Science* **76**: 563.
Thornthwaite CW, Mather. 1957. Instructions and Tables for Computing Potential Evapotranspiration and the Water Balance. Drexel Institute of Technology, Laboratory of Climatology: Centerton; Publications in Climatology, Vol. 10, No. 3, 185–311.

